

行政院國家科學委員會專題研究計畫 成果報告

肖基障金氧半場效体之數值模擬

計畫類別：個別型計畫

計畫編號：NSC90-2215-E-009-063-

執行期間：90年08月01日至91年07月31日

執行單位：國立交通大學電子工程學系

計畫主持人：郭雙發

計畫參與人員：黃琪聰

報告類型：精簡報告

處理方式：本計畫涉及專利或其他智慧財產權，2年後可公開查詢

中 華 民 國 92 年 5 月 21 日

肖基障金氧半場效體之數值模擬

計畫編號：NSC90-2215-E009-063

執行期限：90/08/01~91/07/31

主持人：郭雙發 國立交通大學電子研究所教授

E-mail：sfguo@cc.nctu.edu.tw

計畫參與人員：黃琪聰 國立交通大學電子研究所

一、中文摘要

吾人利用數值方法以模擬分析奈米尺寸的肖基障金氧半場效體的電學特性。針對奈米元件的高電場熱電子效應，吾人直接利用波茲曼傳輸方程式確實地求解通道區的載子能量分佈，而非假設為傳統的波茲曼分佈。至於肖基障的穿隧電流，則採取量子力學模型，利用 Airy 函數直接解薛丁格方程式，此方法確實比採用 WKB 近似法所計算者更為準確。在奈米元件的模擬分析中，帕松方程式與電流連續方程式係與波茲曼傳輸方程式相結合以提供通道區的電場強度、載子濃度及電流密度之正確分佈。

關鍵詞：肖基障金氧半場效體、波茲曼傳輸方程式、Airy 函數、WKB 近似法

Abstract:

The major work of this project is to simulate the electrical characteristics of Schottky barrier MOSFET with gate length in the range of nanometer. Due to high electric field and hot carrier effects in the nanometer devices, the electron distribution function in the channel region is calculated directly by using the Boltzmann transport equations and is not assumed to be the conventional Boltzmann distribution. The tunneling current in the Schottky-barrier is evaluated by the quantum tunneling model coupled with an Airy function approach. Direct solving of the Schrodinger equation gives more accurate results than the conventional WKB approximation. For the simulation of nanometer devices, Boltzmann transport equation is coupled with Poisson equation and current continuity equation. This approach provides more accurate results for the distribution of electric field, carrier concentration and current density in the channel region as well as the terminal I-V and C-V Characteristics.

Keywords: Schottky barrier MOSFET, Boltzmann transport equations, Airy function, WKB approximation.

二、緣由與目的

本計畫主要是採用數值方法模擬肖基障金氧半場效體 (SB-MOSFET) 的電場強度、載子濃度、電流密度之內部分佈及電流-電壓、電容-電壓之外部特性。對於高電場熱載子的奈米元件，吾人需直接求解波茲曼傳輸方程式 (Boltzmann Transport Equation, BTE)。對於能位分佈甚窄的肖基障，則需用量子力學方法解穿隧電流 (Tunneling Current)。

針對肖基障金氧半場效體結構，吾人首先假設金屬矽化物的電氣特性與金屬相同，亦即在金屬矽化物內部為等電位。其次，在金屬/半導體接觸處則形成肖基障，對其穿隧電流，雖可利用 WKB 近似法計算，但此方法忽略了熱離子放射的反射部分，在能障頂端較不準確。所以，此計畫使用 Airy 函數直接求解薛丁格方程式，計算肖基障的熱離子放射和穿隧電流。在金氧半場效體的通道部分，則利用波茲曼傳輸方程式來求解載子的位置和能量的分佈函數 (distribution function)，而非假設為傳統的波茲曼分佈。基本上，在奈米規格閘極長度的通道，吾人假設彈道 (ballistic) 現象並未產生，所以，波茲曼傳輸方程式中的一些散射機制仍可適用。波茲曼傳輸方程式的求解方法，主要採用球諧函數展開 (Spherical harmonic expansion)，只取近似值至一次項。

三、物理模式

The total tunneling currents density crossing the Schottky barrier is a sum of two components: J_{MS} , which is the electrons flowing from metal to semiconductor, and J_{SM} that from semiconductor to metal. They can be calculated as follows:

$$J_{MS} = -\frac{A^*T}{k} \int_0^\infty f_m(\epsilon)[1-f_s(\epsilon)] |T_p(\epsilon)| d\epsilon \quad (1)$$

$$J_{SM} = -\frac{A^*T}{k} \int_0^\infty f_s(\epsilon)[1-f_m(\epsilon)] |T_p(\epsilon)| d\epsilon \quad (2)$$

where $f_m(x)$ and $f_s(x)$ are the Fermi-Dirac distribution functions in metal and semiconductor, respectively. A^* is the effective Richardson constant, T is temperature, k is the Boltzmann constant and $|T_p(x)|$ is the transmission probability of electrons for the barrier.

The key note for calculating the total current density is the transmission probability $|T_p(x)|$. To estimate the transmission probability of a potential barrier shown in Figure 1, it is discretized into n regions and a constant electric field is assumed to be applied to each region. Under this assumption, the

potential energy is a linear function of distance and the Schrodinger equation can be solved directly by using Airy functions. Consider the 1-D time independent Schrodinger equation:

$$-\frac{\hbar^2}{2m} \frac{\partial^2 \Psi}{\partial x^2} + V(x)\Psi = E\Psi \quad (3)$$

Here $V(x)$ in the i^{th} region has the following form:

$$V_i(x) = \frac{V_{iR} - V_{iL}}{W_i} x + V_{iL} = -F_i x + V_{iL} \quad (4)$$

where V_{iR} and V_{iL} are right-side and left-side potential individually in the i^{th} region, W_i is the width of the i^{th} region and F_i is the electrical field of the i^{th} region. Substitute (4) into (3) and solve the Schrodinger equation, the wavefunction of the i^{th} region is

$$\Psi_i(\dots_i(x)) = C_i^+ A(\dots_i(x)) + C_i^- B(\dots_i(x)) \quad (5)$$

where

$$\dots_i(x) = \left(\frac{2m_e F_i}{\hbar^2} \right)^{\frac{1}{3}} (-x + y_i) \quad (6)$$

$$y_i = \frac{1}{F_i} \left(V_{iL} - \frac{E}{e} \right) \quad (7)$$

and e is electron charge.

For continuity of wavefunction, the value of wave-function and its derivative at region's boundary must be satisfied the following conditions:

$$\begin{cases} \Psi_i(W_i) = \Psi_{i+1}(0) \\ \frac{d\Psi_i(x)}{dx} \Big|_{x=W_i} = \frac{d\Psi_{i+1}(x)}{dx} \Big|_{x=0} \end{cases} \quad (8)$$

To deduce the transmission probability, the wave-function in the metal region and n^{th} region are assumed to be

$$\Psi_M = e^{ik_m x} + \text{Re}^{-ik_m x}, \quad k_m = \frac{\sqrt{2m_o E}}{\hbar} \quad (9)$$

$$\Psi_n = T_t e^{ik_n x}, \quad k_n = \frac{\sqrt{2m_o (E - eV_n)}}{\hbar} \quad (10)$$

where m_o is free electron mass and \hbar is the reduced Plank constant.

Using (8), a matrix form is deduced for each region.

$$M_i = \begin{bmatrix} A(\dots_i(0)) & B(\dots_i(0)) \\ S_i A'(\dots_i(0)) & S_i B'(\dots_i(0)) \end{bmatrix}^{-1} \begin{bmatrix} A(\dots_i(W_i)) & B(\dots_i(W_i)) \\ S_i A'(\dots_i(W_i)) & S_i B'(\dots_i(W_i)) \end{bmatrix} \quad (11)$$

Combing all equations resulting from (8), we can get

$$\begin{bmatrix} 1 & 1 \\ ik_m & -ik_m \end{bmatrix} \begin{bmatrix} 1 \\ R \end{bmatrix} = \prod_{i=1}^{n-1} M_i \begin{bmatrix} 1 \\ ik_n \end{bmatrix} T_t \quad (12)$$

In this way the transmission probability T_p is calculated by $T_t \times T_t^*$.

In addition to transmission probability T_p , the distribution function $f_s(E)$ is another key point. The Spherical-Harmonics expansion method is used to solve the Boltzmann transport equation (BTE). A stationary BTE for electrons is

$$u_g(k) \bullet \nabla_r f(r, k) - \frac{q}{\hbar} F(r) \bullet \nabla_k f(r, k) \quad (13)$$

$$= \int S(k', k) f(r, k') dk' - f(r, k) \int S(k, k') dk'$$

where $u_g(k) = \frac{1}{\hbar} \nabla_k E(k)$

The SH expansion of distribution function yields

$$f(r, k) = f_0(r, k) + \frac{k_i}{k} f_1(r, k) + \frac{1}{2} \frac{k_i k_j}{k k} f_2(r, k) + \dots, \quad i, j = 1, 2, 3 \quad (14)$$

Using the first-order approximation and to transform the coordinate (r, k) to (r, H) , where $H = E(k) - q\phi(r)$ is total energy, the resulting BTE reads

$$\frac{\partial}{\partial r_i} \left(g \tau_1 u_g^2 \frac{\partial f_0}{\partial r_i} \right) + 3C_{op} g M_{op} - 3C_{ii} g^2 f_0(E) \quad (15)$$

$$+ 3g \int A(E', E) f_0(E') g(E') dE' = 0$$

$$f_i = -\tau_1 u_g \frac{\partial f_0}{\partial r_i} + \frac{\tau_1}{3} \int B(E', E) f_1(E') g(E') dE'$$

Using the following equations to discretize (15) for 1-D case

$$\frac{\partial H}{\partial x} = -q \frac{\partial \phi}{\partial x} = qE, \quad \frac{\partial f}{\partial x} = \frac{\partial f}{\partial v} qE, \quad \frac{\partial}{\partial x} \left(\frac{\partial f}{\partial x} \right) = (qE)^2 \frac{\partial^2 f}{\partial v^2} \quad (16)$$

$$\frac{\partial f}{\partial v} = \frac{f_{i+1} - f_{i-1}}{2\Delta v}, \quad \frac{\partial^2 f}{\partial v^2} = \frac{f_{i+1} - 2f_i + f_{i-1}}{\Delta v^2} \quad (17)$$

Let $d[\downarrow] = g(i\Delta v) \tau_1 u_g^2 (qE)^2 \frac{1}{\Delta v^2} + 3C_{op} g(i\Delta v) g^- N_{op}^- - \frac{d2(i)}{2\Delta v}$

$$\mathcal{A}[\downarrow] = g(i\Delta v) \tau_1 u_g^2 (qE)^2 \frac{(-2)}{\Delta v^2} + 3C_{op} g(i\Delta v) \quad (18)$$

$$\left[(1 - \dots - N_{op}^-) g^+ - g^-(1 + N_{op}^-) \right] - 3C_{ii} g(v) g(i\Delta v)$$

$$d[\uparrow] = g(i\Delta v) \tau_1 u_g^2 (qE)^2 \frac{1}{\Delta v^2} + 3C_{op} g(i\Delta v) N_{op}^+ - g^+ + \frac{d2(i)}{2\Delta v}$$

$$qq_i = -3g(v) \sum_i A(i\Delta v, v) f_i g_i \Delta v$$

Simplify equation is $d[\downarrow]f_{i-1} + \mathcal{A}[\downarrow]f_i + d[\uparrow]f_{i+1} = qq_i$

where

$$\sim = \frac{\hbar \tilde{S}_{op}}{\Delta v}, \quad N_{op}^+ = N_{op} + 1,$$

$$g^+ = g(i\Delta v + \hbar \tilde{S}_{op}), \quad g^- = g(i\Delta v - \hbar \tilde{S}_{op})$$

$$d2(i) = (qE)^2 \left[\frac{g_{i+1} - g_{i-1}}{2\Delta v} \tau_1 u_g^2 + g u_g^2 \frac{\tau_1 - \tau_{i-1}}{2\Delta v} + 2g \tau_1 u_g \frac{u_{s,i+1} - u_{s,i-1}}{2\Delta v} \right]$$

$$\begin{aligned}
A(E', E) &= \int [S_0^{ii}(E', E, E'') + S_0^{ii}(E', E'', E)] g(E'') dE'' \\
&= \sum_{j=1}^3 \{b_j^{ii} [(a_j^2 + k'^2 + k^2)^2 - 4k'^2 k^2]^{-1} g(E'') \\
&\quad + b_j^{ii} [(a_j^2 + k'^2 + k''^2)^2 - 4k'^2 k''^2]^{-1} g(E'')\}
\end{aligned} \tag{19}$$

Extending the above results to 2-D case, it can be formulated as following:

$$h_i = x_{i+1} - x_i, \quad k_j = y_{j+1} - y_j, \quad iv = \frac{\hbar S_{op}}{\Delta V}$$

Let

$$\begin{aligned}
tempd(i, j, \ell) &= \frac{-2F_{i,j,\ell}}{h_i(h_{i-1} + h_i)} g_{i+\frac{1}{2},j,\ell} \dagger_{i+\frac{1}{2},j,\ell} u_{g_{i+\frac{1}{2},j,\ell}}^2 \\
tempk(i, j, \ell) &= \frac{-2F_{i,j,\ell}}{h_{i-1}(h_{i-1} + h_i)} g_{i-\frac{1}{2},j,\ell} \dagger_{i-\frac{1}{2},j,\ell} u_{g_{i-\frac{1}{2},j,\ell}}^2 \\
tempd(i, j, \ell) &= \frac{-2F_{i,j,\ell}}{k_j(k_{j-1} + k_j)} g_{i,j+\frac{1}{2},\ell} \dagger_{i,j+\frac{1}{2},\ell} u_{g_{i,j+\frac{1}{2},\ell}}^2 \\
tempd(i, j, \ell) &= \frac{-2F_{i,j,\ell}}{k_{j-1}(k_{j-1} + k_j)} g_{i,j-\frac{1}{2},\ell} \dagger_{i,j-\frac{1}{2},\ell} u_{g_{i,j-\frac{1}{2},\ell}}^2 \\
tempk(i, j, \ell) &= 3C_{op} g_{i,j,\ell} (N_{op} g_{i,j,\ell+iv} + N_{op}^* g_{i,j,\ell-iv}) + 3C_{ii} g_{i,j,\ell} g_{i,j,\ell} \\
dd(i, j, \ell) &= tempd(i, j, \ell) + tempk(i, j, \ell) + \\
&\quad tempk(i, j, \ell) + tempd(i, j, \ell) - tempk(i, j, \ell)
\end{aligned}$$

$$\begin{aligned}
F_{i,j,\ell+iv} &= (1 + [iv] - iv) F_{i,j,\ell+[iv]} + (iv - [iv]) F_{i,j,\ell+[iv]+1} \\
&= sa F_{i,j,\ell+[iv]} + sb F_{i,j,\ell+[iv]+1} \\
F_{i,j,\ell-iv} &= (1 + [iv] - iv) F_{i,j,\ell-[iv]} + (iv - [iv]) F_{i,j,\ell-[iv]-1} \\
&= sa F_{i,j,\ell-[iv]} + sb F_{i,j,\ell-[iv]-1} \\
u1(i, j, \ell) &= 3C_{op} g_{i,j,\ell} N_{op}^* g_{i,j,\ell+iv} \bullet sa \\
u2(i, j, \ell) &= 3C_{op} g_{i,j,\ell} N_{op}^* g_{i,j,\ell+iv} \bullet sb \\
L1(i, j, \ell) &= 3C_{op} g_{i,j,\ell} N_{op} g_{i,j,\ell-iv} \bullet sa \\
L2(i, j, \ell) &= 3C_{op} g_{i,j,\ell} N_{op} g_{i,j,\ell-iv} \bullet sb
\end{aligned}$$

The discretized equation can read

$$\begin{aligned}
[dd(i, j, \ell) + u1(i, j, \ell) + L1(i, j, \ell)] F_{i,j,\ell} \\
+ u2(i, j, \ell) F_{i,j,\ell+1} + L2(i, j, \ell) F_{i,j,\ell-1} = QQ_\ell
\end{aligned}$$

where

$$\begin{aligned}
QQ_\ell &= -3g_{i,j,\ell} \Sigma A_{i,\ell} F_{i,j,\ell} g_{i,j,\ell} \Delta V + tempd(i, j, \ell) F_{i+1,j,\ell} \\
&\quad + tempk(i, j, \ell) F_{i-1,j,\ell} + tempd(i, j, \ell) F_{i,j+1,\ell} + tempd(i, j, \ell) F_{i,j-1,\ell}
\end{aligned} \tag{20}$$

The scattering mechanisms are impact ionization and the collisions with acoustic phonons, optical phonons, and ionized impurities. All scattering parameters are from [7],[8].

四、結果與討論

For the parabolic shape of potential barrier shown in figure 1, the calculated results of the transmission probability T_b using the methods of Airy function and WKB approximation are given in figure2 and figure3. We find that the transmission probability obtained by the WKB methods is under-estimated for all applied voltage at low electron energy. However, it is over-estimated at high electron energy near the peak of potential barrier. We also note that the number of discreted regions is not necessary to be large to seek for exact solution. Ten regions are good enough to give exact solution.

Figure 4 is the total electron-phonon scattering rate and Figure 5 is the impact ionization scattering rate for electrons. All of them are calculated by using the parameters of [7], [8] and are substantial consistent with [7]. Figure 6 gives the distribution function in a NMOS device near the channel surface by solving (20). This result verifies that the codes of full-band spherical harmonics expansion for solving BTE are well done. By summation of density of state and distribution function multiplication gives the electron concentration. Figure 7 shows that the electron concentration distribution under various depths. Under the channel, the electron concentrations reduce more quickly with depth. Upon these conditions, we can estimate the inversion layer thickness.

五、結論

The numerical method developed in this work to solve the Schrodinger equation in a potential barrier using the Airy function is more accurate and flexible than the WKB approximation. Using full-band spherical harmonics expansion methods, we can solve the BTE incorporate with many scattering mechanisms. However, it is a tedious work to solve the 2-D BTE. The coupling of Poisson equation with current continuity equation will be left as a feature work.

六、參考文獻

- [1] M.P.Lepselter and S.M.Sze, "SB-IGFET: An Insulated-Fate Field-Effect Transistor Using Schottky Barrier Contacts for Source and Drain," *Proc. IEEE* vol. 56, pp.1400, 1968.

- [2] J.R.Tucker, et al., "Extended Abstracts of the 1994 Int.Conf. On Solid State Devices and Materials (SSDM'94)," Japan Society of Applied Physics, pp322-324, 1994.
- [3] J.P.Snyder, C.R.Helms, Y.Nishi," Experimental Investigation of a PtSi Source and Drain field emission transistor," *Appl. Phys. Lett.* Vol.67, pp1420-1422, 1995.
- [4] C.Wang, J.P.Snyder, and J.R.Tucker," Sub-40 nm PtSi Schottky source/drain metal-oxide- semiconductor field-effect transistors," *Appl. Phys. Lett.*, vol.74, pp.1174-1176, 1999.
- [5] J.R.Tucker, Advanced Workshop on Frontiers in Electronics, WOFE '97, pp.97-100, 1997.
- [6] K.F.Brennan and C.J.Summers," Theory of the Resonant Tunneling in a Variably Spaced Multi-Quantum Well Structure: An Airy Function Approach," *J. Appl. Phys.*, vol. 61, pp.614-623, 1987.
- [7] Maria Cristina Vecchi and Massimo Rudan," Modeling Electron and Hole Transport with full-band structure effects by means of the spherical-harmonics expansion of BTE," *IEEE trans. Electron Devices*, vol. 45, pp230-238, 1998.
- [8] Susanna Reggiani, Maria Cristina Vecchi and Massimo Rudan," Investigation on Electron and Hole Transport properties using the full-band spherical-harmonics expansion method.

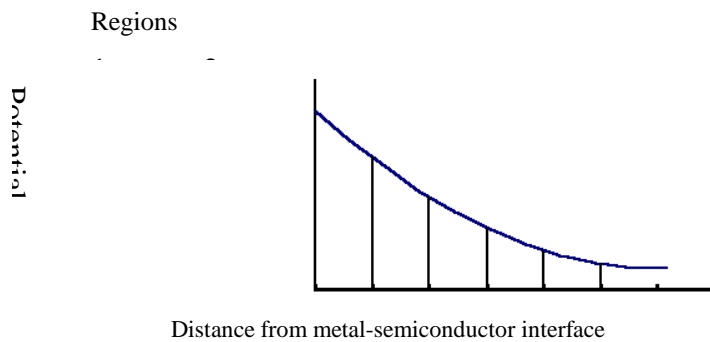


Figure 1. Discretization of a potential barrier.

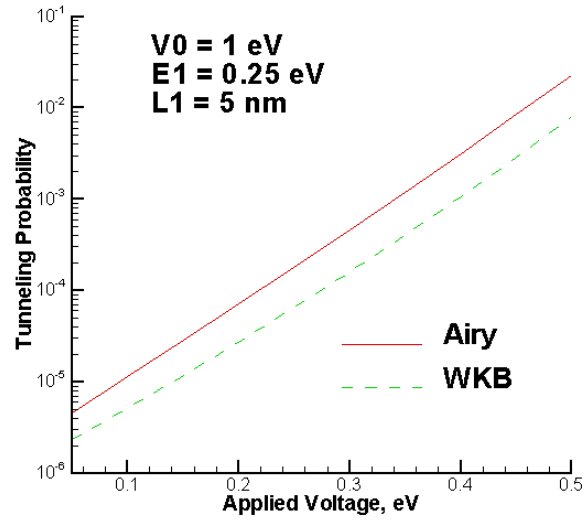


Figure 2. Tunneling probability vs. applied voltage for a typical potential barrier using Airy function and WKB approximation.

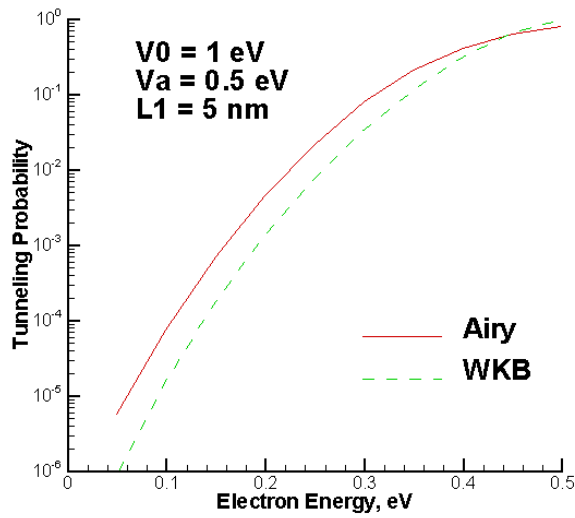


Figure 3. Tunneling probability vs. electron energy for a typical potential barrier using Airy function and WKB approximation.

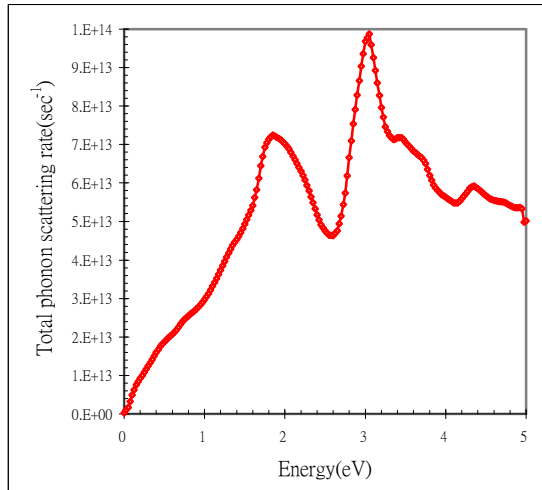


Figure 4. Total electron-phonon scattering rate

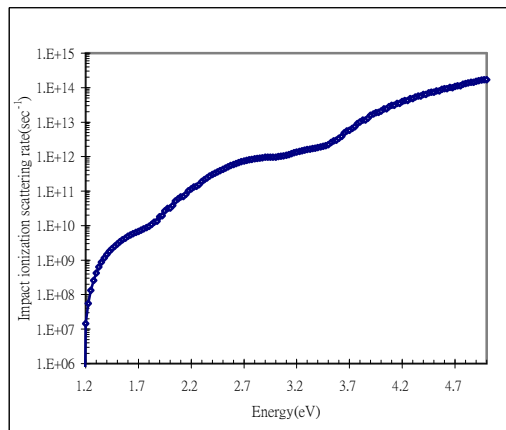


Figure 5. Impact ionization scattering rate for electrons.

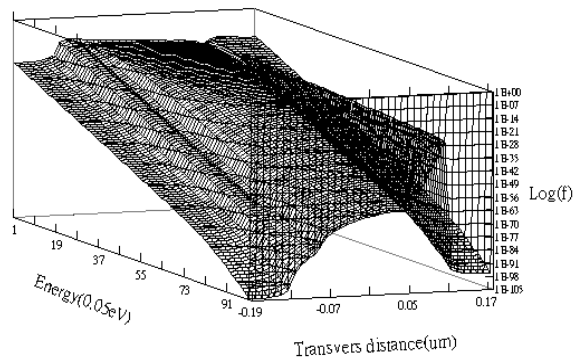


Figure 6. The distribution function along the channel $0.007\mu\text{m}$ below the surface. The applied bias is $V_{\text{GS}}=V_{\text{DS}}=3\text{Volts}$.

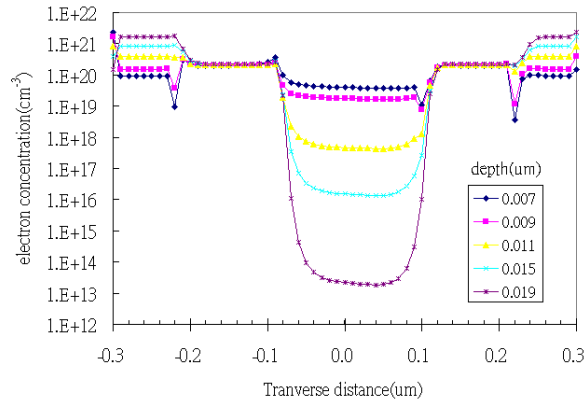


Figure 7. The electron concentration under varies depths.